C/ORNL 94-0358

ORNL/M--6598

ornl

OAK RIDGE NATIONAL LABORATORY

LOCKHEED MARTIN

MANAGED AND OPERATED BY
LOCKHEED MARTIN ENERGY RESEARCH CORPORATION
FOR THE UNITED STATES
DEPARTMENT OF ENERGY

ORNL-27 (3-96)

CRADA Final Report
for
CRADA Number ORNL94-0358

MANUFACTURE OF DIE CASTING DIES BY HOT ISOSTATIC PRESSING

S. Viswanathan, W. Ren, and K. Luk
Oak Ridge National Laboratory
Oak Ridge, Tennessee

H. G. Brucher
Doehler-Jarvis
Toledo, Ohio

Date Published: September 1998

Prepared by the
Oak Ridge National Laboratory
Oak Ridge, Tennessee 37831
managed by
Lockheed Martin Energy Research Corporation
for the
U.S. Department Of Energy
under contract DE-AC05-96OR22464

APPROVED FOR PUBLIC RELEASE

UNLIMITED DISTRIBUTION

CONTENTS

Abstract

The reason for this Cooperative Research and Development Agreement (CRADA) between the Oak Ridge National Laboratory (ORNL) and Doehler-Jarvis was to investigate the manufacture die-casting dies with internal water-cooling lines by hot-isostatic pressing (HIPing) of H13 tool steel powder. The use of HIPing will allow the near-net-shape manufacture of dies and the strategic placement of water-cooling lines during manufacture. The production of near-net-shape dies by HIPing involves the generation of HIPing diagrams, the design of the can that can be used for HIPing a die with complex details, strategic placement of water-cooling lines in the die, computer modeling to predict movement of the water lines during HIPing, and the development of strategies for placing water lines in the appropriate locations. The results presented include a literature review, particle analysis and characterization of H13 tool steel powder, and modeling of the HIPing process.

CRADA Objective

The objective of this project was the development of die casting dies by (HIPing). The use of HIPing for the manufacture of dies will allow the near-net-shape manufacture of dies, resulting in reduced manufacturing costs. In addition, the use of HIPing would allow the strategic placement of water cooling lines during manufacture and the option to use corrosion-resistant piping for water cooling, resulting in increased die life, reduced distortion during operation, and increased production rates. Further development of HIPing for die manufacture could include the incorporation of advanced materials in specific areas to further improve die performance.

Assessment of CRADA

The results of the powder characterization and modeling studies undertaken in this project suggested the feasibility of the production of near-net-shaped dies by HIPing. However, further experimental trials involving the design of the can that can be used for HIPing a die with complex details and the strategic placement of water cooling lines in the die is needed. Since the water lines may move during HIPing, computer modeling must be used to predict movement of the water lines and devise strategies for placing water lines in the appropriate locations. Unfortunately, the level of effort allowed in this CRADA did not allow further experimental and computer trials.

CRADA Benefit to DOE

This CRADA has enhanced the capabilities and skills at ORNL in the areas of HIPing process design, process modeling, and the development of HIPing diagrams. This will improve the prospects of future projects dealing with HIPing or powder consolidation. The experience gained in this project could be applied to the development of near-net shape dies for the processing of advanced materials.

This work was supported through a Cooperative Research and Development Agreement with Doehler-Jarvis, Toledo, Ohio, sponsored by the Laboratory Technology Research Program, Office of Energy Research, U.S. Department of Energy, under contract DE-AC05-96OR22464 with Oak Ridge National Laboratory, managed by Lockheed Martin Energy Research Corporation.

The CRADA also successfully demonstrated the application of the Department of Energy (DOE) technologies in the areas of process modeling and the development of novel processes. It has also demonstrated that DOE programs can allow industry to access the technology available at DOE laboratories.

Technical Discussion

The primary advantages of a powder technology are:

1. The production of complex compositions without the severe chemical segregation observed in conventional ingot processing.
2. The confinement of the solidification of the powder to a fine powder particle rather than a large casting to overcome segregation.
3. The attainment of an ultrafine grain size and superior homogeneity by solidification of the powder an order of magnitude faster than that of a casting.

During HIPing, the densification of a powder compact can be divided into three steps [1]:

1. Particle rearrangement (i.e., the formation of interparticle bonds by interparticle movement at low pressures). It occurs at the beginning of a HIPing process.
2. Plasticity (i.e., rapid deformation by plastic yielding, athermal plastic flow such that points of contact are expanded to areas of contact) occurring at low temperatures ($T < 0.3\ T_m$, where T_m is the melting point or solidus temperature).
3. Time-dependent deformation processes such as power law creep, Nabarro-Herring and Coble creep, and volume and interparticle boundary diffusion, occurring at high temperatures ($T \approx 0.65\ T_m$).

A typical HIPing process involves [2]:

1. Production of fine powder via gas atomization.
2. Classification of the powder by screening.
3. Obtaining desired composition through blending, where necessary.
4. Filling the powder into carbon steel or stainless steel containers (about 65% of theoretical density). The mold size is determined by adding overstock onto finished dimensions. Fill stems are welded onto the container for powder loading [2]. The container is leak checked to ensure a hermetical seal [2]. Charges of several tons have been reported [3].
5. Evacuating the powder-filled containers.
6. Sealing the fill stems via hot-stem crimping to maintain vacuum in the compact.
7. Consolidating the compact to full density by HIPing.
8. Removing the containers by machining or acid pickling.
9. Finishing the parts by machining.

The basic parameters for a HIPing process are temperature, pressure, and hold time. The goal is to achieve compacts of theoretical density free of defects and with desirable microstructures. HIPing cycles should be selected based on the alloy and property requirements. Generally, the cycle is determined by trial and error. As a rough estimation, the HIPing temperature can be two-thirds of the melting point of the material [4]. Table 1 lists some typical materials processed by HIPing and their HIPing parameters. A typical cycle for tool steel-type materials from Table 1 is: 1129°C (2065°F) at 100 MPa (15 ksi) for 4 h [ref. 2]. Efforts have been made to model the densification process in the hope of optimizing HIPing diagrams. For example, HIPing diagrams are optimized through the construction of mechanism maps that model the microdensification processes [4]. Results

indicate that increasing temperature or pressure increases the density. For metals, the temperatures used are usually close to their melting temperatures and, therefore, increasing pressure is preferred; for ceramics, increasing temperature is preferred.

Some optional parameters include:

1. Particle Size: It is known from the mechanism maps that final theoretical density is achieved by solid diffusion, usually at high temperatures. Therefore, small particle size is preferred [4,5]. On the other hand, at low temperatures, densification is controlled by bulk flow, and big grain size lowers the flow stress and, thus, increases the rate of densification [5].
2. Particle Shape: Irregular powders have greater coordination and rate of contact growth than spherical powders, especially at high pressures. Therefore, they are desired for better densification behavior [1].
3. Second Hold Time: A second hold period, within a single cycle, in order to optimize the as-HIPed microstructure is employed in some cases [3]. The compacts are held at a certain temperature, and pressure for a required period of time immediately after the densification is completed to allow desired microstructures to form.
4. Inert Gas: Inert gases are sometimes used to minimize surface reactions of the powder [3].
5. Cold Work: Cold work on the surface of metal powders can promote consolidation and lead to a fine grain structure as a result of localized recrystallization [3].
6. Pressurization Rate: Rate of pressurization can be increased to influence resultant material properties [3].
7. Pressure Amplitude: High pressure is reported to stabilize austenite and decrease self-diffusion in carbon steels [3]. Pressure effects are also reported on the transformation of a second phase in titanium alloy and stainless steels. HIPing of rapidly solidified Ti-6Al-4V powder at 3000 atm did not result in the expected partial transformation of alpha to beta, which would occur during subsequent heating at atmospheric pressure, indicating that the alpha phase originally present in the powder was stabilized by the pressure during HIPing. For stainless steels, it has been suggested that the reduction in delta ferrite content of stainless weld metal is considerably enhanced by the pressure applied during HIPing process. A study of the response of a 3Cr-Mo steel (EN 40B) to HIPing indicated that both the as-HIPed hardness and tensile properties after subsequent tempering were improved, suggesting that the transformation to martensite and bainite during post-HIP cooling was more extensive than expected [3].

Anisotropic shrinkage is possible due to effects related to the part geometry [2]. In general, the surface gets hot first and sinters faster than the interior, giving a denser skin which, in turn, conducts heat faster and further increases the temperature difference. Under some conditions, a densification front develops and propagates inward and, thus, causes large shape changes [6]. The factors controlling anisotropic shrinkage are:

1. Heating and pressurization rates prior to the HIP hold cycle.
2. Material properties of the powder and the container as a function of temperature, density, and part geometry.
3. Position of welds in the container.

In the case of bimetallic parts, cracking could result due to the incompatibility of alloy compositions and heat treatments. To solve these problems, the trial and error method is still popularly employed. However, efforts have been made to attack the problems more scientifically through the following approaches:

1. Empirical Modeling (for simple shapes) [2]:
   (a) Analyzing dimensional data from before and after HIP for representative product shapes.
   (b) Generating fitting curves of dimensional shrinkage as a function of some geometrical parameters (e.g., aspect ratio, surface area ratio).
   (c) Calculating the overstock with a computer based upon the curves.

2. Numerical Modeling (for complex shapes) [2]:
   (a) Obtaining the material property data as a function of temperature and density.
   (b) Evaluating HIP shrinkage based upon continuum mechanics equations solved by the finite element method (FEM).

3. Microstructure-Based Process Modeling [7]:
   (a) Describing the densification and deformation behavior of a particulate porous compact.
   (b) Incorporating the behavior into FEM-based models to predict shape changes for different process cycles.

For the purpose of quality control, it is very important to be able to monitor the HIPing process and quantitatively measure product and quality. Eddy-current sensing can give detailed information about the densification of HIP samples. In this way, it is possible to monitor the HIP process in real time. A sensor system operating at 1100°C has been reported [7,8]. Final relative density and percent interconnected porosity can also be measured according to ASTM B-328. Quantitative metallographic methods, such as point counting or line intersection, can be used to determine the particle-particle contact area. A circle can be used as the test line to avoid questions about the end points of a line. The value of particle-particle contact area, or the 'contiguity' (C_m) of the metal powder particles, is given by [1]:

$$C_m = 2P^{mm}{}_L/(2P^{mm}{}_L + P^{mp}{}_L) , \qquad (1)$$

where

$P^{mm}{}_L$ = number of intersections with the metal-metal contact surface/length of test line.

$P^{mp}{}_L$ = corresponding number of intersections with metal-pore surface.

Materials and their HIPing parameters found in the literature are summarized in Table 1. Some of the materials have similar chemical compositions as H13 tool steel. These data can be used as references in designing the HIPing diagram.

Project Description and Results

The results presented includes particle analysis and characterization of H13 tool steel powder and analytical modeling of the HIPing process.

Table 1. Some materials processed by hot-isostatic pressing (HIPing) and their HIPing parameters

Material	Fe	Cr	Mo	Si	V	Mn	C	Ni	Cu	P	S	Other	HIP condition
H13	Bal.	5.25	1.36	1.12	0.88	0.44	0.41	0.12	0.11	0.007	< 0.005	---	
CPM 10V	Bal.	5.25	1.3	0.9	9.75	0.5	2.45	---	---	---	---	---	1129°C/100 MPa /4 hr.
MPL -1	Bal.	0.24	3.0	0.7	9.0	0.5	3.75	---	---	---	---	---	Similar
Rene 95	---	13.0	3.5	---	---	---	0.06	Bal.	---	---	---	8.0Co/3.5W/3.5Nb/ 3.5Al/ 2.5Ti/0.01B/0.05Zr/	Similar
Alloy 625	1.4	21.0	9.0	---	---	---	0.025	Bal.	---	---	---	4.0Nb/0.3Al/0.2Ti/	Similar
Alloy 625M	5.0	20.5	8.7	---	---	---	0.03	Bal.	---	---	---	5.0Nb/0.5Al/0.1Ti/	Similar
Low carbon Astroloy	---	15.0	5.0	---	---	---	0.03	Bal.	---	---	---	17.0Co/4.0Al/3.5Ti/ 0.02B/0.04Zr/	Similar
Tool steels	Bal.	~ 4.0	5.0 - 7.0	---	3.1 - 6.5	---	1.3 - 2.3	---	---	---	---	~6.5W/(8.5 - 10.5)Co/	1200°C/150 MPa/1 h
Superalloys													996-1213°C 70-180MPa 1-4 h
Alumina													1200-1400°C 100-200MPa 2-4 h
Ice													0.32-3.62 MPa

Particle Analysis of H13 Powder

Analysis of the H13 powder supplied by Doehler-Jarvis was conducted using both standard sieve analysis and an L&N Microtrac. The results are given in Tables 2 and 3, respectively.

Table 2. Size distribution of H13 powder by U.S. standard sieve analysis

U.S. standard mesh size	Particle size (μm)	Percent (wt)	U.S. standard mesh size	Particle size (μm)	Percent (wt)
-70/+80	205[a]/+177	0.0	-200/+230	-74/+63	10.2
-80/+100	-177/+149	1.1	-230/+270	-63/+53	7.1
-100/+120	-149/+125	5.5	-270/+325	-53/+44	8.9
-120/+140	-125/+105	7.0	-325/+400	-44/+37	9.0
-140/+170	-105/+88	8.9	-400/+500	-37/+28[a]	11.2
-170/+200	-88/+74	12.3	-500	-28[a]	18.7

[a] Estimated values.

Sieve analysis is given by the weight percent of particles either passing through or retained by a given sieve. For example, sieve analysis shows that all particles of H13 powder passed through U.S. standard mesh size No. 80 (i.e., they are all greater than 177 μm in diameter) and 1.1 wt % of the total particles are between the standard mesh size of Nos. 80 and 100 (i.e., between 177 and 149 μm), and 18.7 wt % of the total particles are smaller than the standard mesh size No. 500. To achieve a dense green compact, a size distribution is needed such that the small particles can fill the spaces among big ones. Thus, the 18.7 wt % of small particles are valuable for densification.

The L&N Microtrac Particle Size Analyzer measures particle size distribution in terms of the volume of particles passing through or retained in each of several size channels. Adjacent channels generally have a common size ratio of $\sqrt{2}$. Particle analysis is given as the volume of particles retained or passing a given channel. For example, the result of Microtrac analysis on the H13 powder shows that 100% of H13 powder particles are smaller than 176 μm in diameter, but only 85% are smaller than 125 μm. Therefore, particles between 176 and 125 μm in diameter are 14.7% of the total particle volume. The average size of the particles is calculated by the means of a volume mean diameter as well as area mean diameter. For the H13 powder, the volume mean diameter is reported as 74.27 μm, while the area mean diameter is given as 48.40 μm. The volume mean diameter of the average particle size is regarded to be more representative for this technique.

Table 3. Size distribution of H13 tool steel by Microtrac analysis

Uncalibrated Sample Volume Data: dV = 0.2095
10th Percentile: %10 = 22.32 (μm)
50th Percentile: %50 = 66.15 (μm)
90th Percentile: %90 = 141.22 (μm)
Mean Diameter of the Volume Distribution: MV = 74.27 (μm)
Calculated Surface Area: CS = 0.124 (m^2/cc)
Standard Deviation: STD.DEV. = 46.93
Area Mean Diameter: MA = 48.40

Channel	Percent passing		Percent retained	
(μm)	Cumulative	Volume	Cumulative	Volume
176	100.0	14.7		
125	85.3	19.4	14.7	14.73
88	65.9	18.9	34.1	19.4
62	47.0	17.4	53.0	18.9
44	29.6	11.3	70.4	17.4
31	18.3	8.6	81.7	11.3
22	9.7	6.5	90.3	8.6
16	3.2	3.2	96.8	6.5
11	0.0	0.0	100.0	3.2
7.0	0.0	0.0	100.0	0.0
5.5	0.0	0.0	100.0	0.0
3.9	0.0	0.0	100.0	0.0
2.8	0.0	0.0	100.0	0.0
1.9	0.0	0.0	100.0	0.0
1.4	0.0	0.0	100.0	0.0
0.9	---	---	100.0	0.0

Optical Characterization of H13 Powder

Optical metallography of the H13 powder was conducted on a polished pellet of compacted powder mounted in epoxy. Specimens were rough ground on Nos. 120 and 600 grit paper followed by 6-μm diamond paste. The final polishing was conducted with 0.05 μm alumina suspension on a polishing cloth. The specimens were etched before observation. The result, shown in Fig. 1, indicates that the particles are spherical with some internal substructure formed during solidification. Figure 2 shows spherical holes observed in two particles formed due to solidification shrinkage. The holes in the particles may have some effect on densification during HIPing. Figure 3 shows a typical particle distribution of the H13 powder.

Process Modeling

Model Development. Theoretical modeling can usually provide guidelines for experimentation as well as part consolidation and, consequently, save time and material. Several methods have been developed to model the HIPing process. For the purposes of modeling, the HIPing densification process is generally divided into two stages, with the relative density (D) and its time derivative ($\dot{D}$) as process variables. D is defined as the ratio of the instantaneous density ρ and the theoretical solid density (ρ_s). $\dot{D}$ is referred to as the densification rate. The objective of an analysis is to determine, as a function of time, the relative density (D) for a given material and operating conditions (pressure and temperature). Uniform spherical particles are assumed in the model.

The initial densification stage is characterized by a relative density (D) of less than 0.9. It is assumed that random dense packing is already attained, and that the starting density is D_0 = 0.64. Consequently, the initial densification stage covers the density range from $D = D_0$ to $D = 0.9$.

At this stage, the individual particles are recognizable entities. The particles are in contact with their neighbors. Overlapping regions are formed between particles, and the circles of overlaps are the necks between particles. During HIPing, the overlapping volumes are redistributed into the void space between particles. The application of pressure can accelerate this overlapping process and reduce the void space. As a particle makes contact with more neighboring particles, the number of contacts increases. The redistribution of the overlapping volumes and the increase in the number of contacts produce a denser material.

In the final densification stage ($0.9 < D < 1$), the particles are no longer recognizable as individual entities. The material is treated as a medium with void spaces. For analysis purposes, the void spaces are modeled as uniformly distributed closed pores, spherical in shape, and equal in size. Densification in the final stage is achieved by the closing of the spherical pores.

In the Monosize Spherical Particle Densification model [1], it is assumed that the particles are monosize spheres initially packed to a random dense relative density of 0.64, and that the initial coordination number is 7.3. The assumed relative density and coordinate number correspond to the numbers for a regular packed array of spheres. During the HIPing process, the particles undergo a uniform deformation and finally eliminate a stack of irregular polyhedral pores at full density.

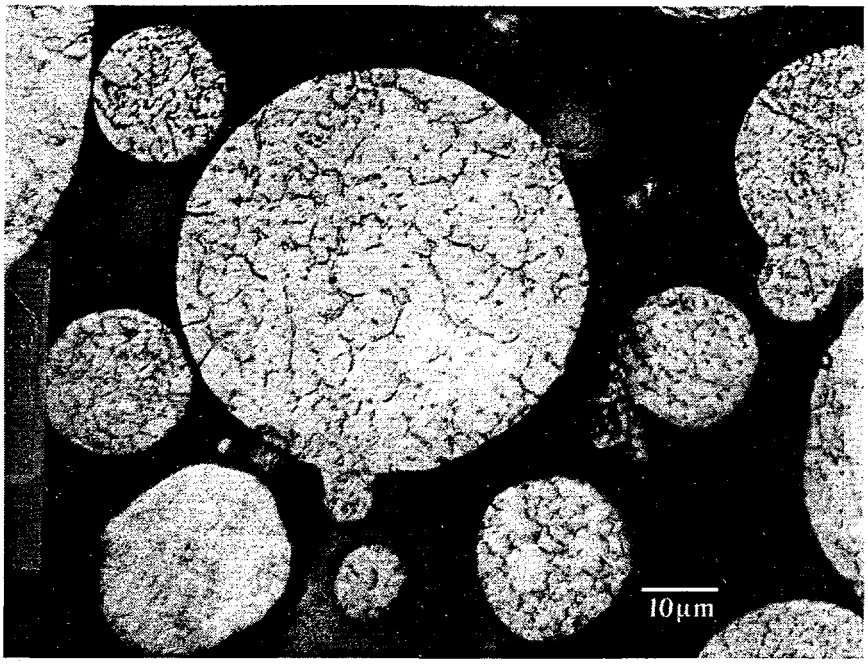

Fig. 1. Micrograph of H13 powder particles indicating a cast microstructure.

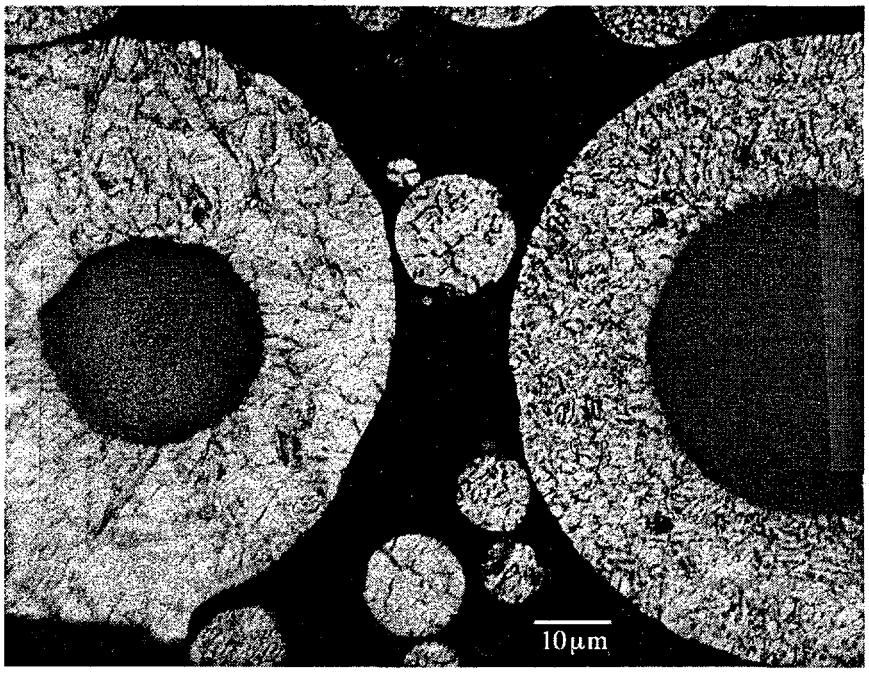

Fig. 2. Spherical holes observed in two particles, indicating that some particles are hollow.

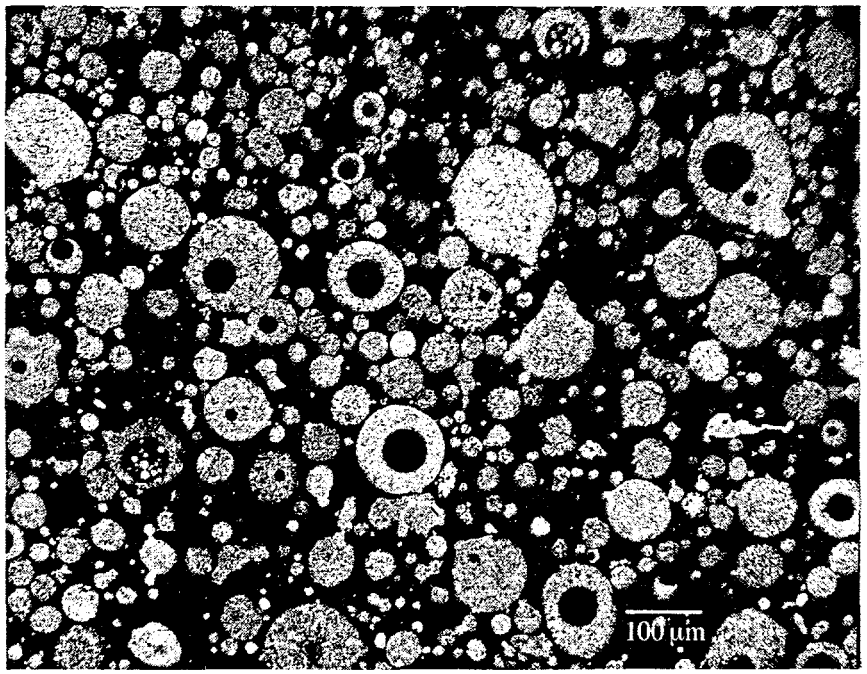

Fig. 3. Typical particle distribution observed in the metallographic sample of H13 powder.

In the Bimodal Particle Size Distribution model [1], it is assumed that yielding and power-law creep are densification mechanisms for two different average particle sizes, and the HIPing process is modeled by weighing the densification behavior of the two particle sizes. It is assumed that forces on all interparticle contacts are equal, and the contact area and coordination development are examined during the HIPing process. The results show that small particles have a larger percentage of contacting surface area than big ones, implying higher interparticle contact stresses on small particles.

Analytical expressions have been derived in the zero-dimension model for density after plastic deformation, the densification rate due to dislocation creep, the densification rate due to Nabarro-Herring-Coble creep, and the densification rate due to vacancy diffusion along grain boundaries of particles and pores. The total densification rate is the sum of the densification rates due to separate mechanisms. In the one-dimensional model, the density nonuniformity occurs due to the inhomogeneity of the temperature field, and the temperature field is predicted by a numerical technique such as the finite element method (FEM) [9].

A model based on grain growth during the HIPing process has also been developed [5]. In the Grain Growth Model, the relationships of grain size versus time-dependent plastic flow and temperature are first derived. Then diffusion grain growth law is derived from Einstein relation, and relationships between densification rate and grain size is obtained. These relationships are different depending on whether pores are open (stage 1) or isolated (stage 2).

An understanding of the operating mechanisms in the HIPing process under different conditions may be understood by constructing a mechanism map using the various densification rate equations [4]. Usually the mechanism maps are presented in three fashions: (1) density versus homologous temperature T/T_m at a fixed pressure p, (2) density versus normalized pressure $p/\sigma_y(T)$ at a fixed T, and c) p versus T at a fixed density.

Because of its nature, the HIPing process is difficult to model. During HIPing, both hydrostatic and deviatoric stress components can cause localized shear stresses and affect the Von Mises yield surface, and cause the Von Mises yield surface to move to higher levels of deviatoric and hydrostatic stress combinations as the metal powder compact "hardens", and both shape and volume changes occur during yielding [10]. When the finite element method is employed, constant remeshing is usually needed during compaction. Problems can also arise from the irregular and changing powder shapes, size distribution, and the change in coordination of powder particles.

Efforts have been made to solve these problems. The elasto-plastic constitutive equations for metal powder deformation have reportedly been incorporated into the finite element method [10], the modified yield surface equation for porous copper has been obtained through test results [11], and an expression for the contact area as a function of relative density has been derived [1]. Equipment has also been developed to study powder behavior and provide data for modeling. For example, an experimental setup termed the Advanced Metalworking System permits direct, indirect, hydrostatic extrusion, isostatic compaction, and triaxial compaction to provide stress versus strain curves of metal powders [3,10].

Densification Mechanisms. Densification by plastic yielding is an instantaneous or time-independent mechanism. Under the action of the applied pressure, a contact stress is developed in the neck region. When the contact stress exceeds the yield stress of the particle material, the particles deform by plastic yield. The overlapping region is increased and, thus, increasing the relative density of the material. Note that this is a self-correcting mechanism. When the particles deform plastically, the contact area is increased, and for a constant applied pressure, the contact stress is reduced. When the contact stress falls below the yield stress, densification by plastic yielding will cease.

The densification attained by plastic yield is used as the starting density for other time-dependent densification mechanisms. The starting relative density is calculated in the following manner:

The average contact area, *a*, is given by:

$$a = \frac{\pi}{3}\frac{(D - D_0)}{(1 - D_0)}R^2, \chi = \sqrt{\frac{a}{\pi}} \quad , \tag{2}$$

where

R = initial particle radius.
D_0 = random dense packing relative density, 0.64.
χ = neck radius.

Let Z be the number of contact neighbors per particle, then total contact area per particle is (aZ). Furthermore, Z is approximated by the equation:

$$Z = 12D \quad . \tag{3}$$

When an external pressure, P, is applied to the compact, the average force in the contact region (f) is given by:

$$f = \frac{4\pi R^2 P}{ZD} \quad . \tag{4}$$

The average contact pressure, P_{eff}, is given by:

$$P_{eff} = \frac{t}{a} = \frac{4\pi R^2 P}{aZD} \quad , \tag{5}$$

which can be simplified to:

$$P_{eff} = \frac{P(1-D_0)}{D^2(D-D_0)} \quad . \tag{6}$$

The yielding criterion is:

$$P_{eff} \geq 3\sigma y \quad , \tag{7}$$

where σy is the yield stress of the compact material.

Let Py be the applied pressure that will just cause yield, then

$$\frac{Py(1-D_0)}{D^2(D-D_0)} = 3\sigma y \tag{8}$$

or

$$Py = \frac{3D^2(D-D_0)}{(1-D_0)} = \sigma y \quad . \tag{9}$$

Alternatively, for a given P, the relative density that can be achieved by plastic yielding (D_{py}) can be solved by:

$$P = \frac{3D_{py}^2(D_{py}-D_0)}{(1-D_0)}\sigma y \quad . \tag{10}$$

Successive iterations are needed to solve for D_{py} .

The above discussions are valid in the initial densification stage. For completeness, the very rare case of plastic yielding in the final stage will be addressed. The yielding now refers to the yielding of the thick shell surrounding the spherical pores.

$$Py = \frac{2\sigma y}{3}\ln\left(\frac{1}{1-D}\right), D \geq 0.9 \tag{11}$$

$$D_{py} = 1 - \exp\left(-\frac{3}{2}\frac{P}{\sigma y}\right) \tag{12}$$

In either case, D_{py} is treated as the starting relative density for the time-dependent densification mechanisms.

When densification occurs by diffusion from interparticle boundaries, diffusion of material can take place across the contact areas between particles. As a result, the particles move closely together, and the void spaces between them are filled. The material becomes denser.

Initial stage densification rate (D_D) is given by:

$$\dot{D}_D = \frac{12 D^{\frac{1}{3}} D_0^{\frac{2}{3}} \left(\delta D_b + \rho D_v\right)}{\left[g(D)\right] kTR^3} Z\Omega P_{eff} \quad , \tag{13}$$

where

δD_b = boundary diffusion factor = $\delta D_{0b} \exp\left[-\frac{Q_b}{R_g T}\right]$.

ρ = curvature of the neck = $\frac{\chi^2}{2(R-\chi)}$.

Dv = lattice diffusion factor = $D_{0v} \exp\left[-\frac{Q_v}{R_g T}\right]$.

Ω = Burger's vector.

g(D) = $\left[\left(\frac{D}{D_0}\right)^{\frac{2}{3}} - 1\right]\left\{2Z_0 + C\left[\left(\frac{D}{D_0}\right)^{\frac{1}{3}} - 1\right]\right\}$.

Z_0 = $12 D_0$ = 7.68.
C = 15.5, the slope of the radial distribution function describing the arrangement of the particle centers.
k = Boltzmann's constant = 1.38×10^{-23} (J/°K).
T = temperature in °K.
R_g = the universal gas constant = 8.31 (J/(mol °K)).

For tool steel:

δD_{0b} = 2×10^{-13} (m^3/s).
Q_b = 167 (kJ/mol).
Ω = 2.58×10^{-10} (m).
$D_0 v$ = 3.7×10^{-5} (m^2/s).
Q_v = 280 (kJ/mol).

Final stage densification rate $\left(\dot{D}_D\right)$ is given by:

$$\dot{D}_D = 54 \frac{\Omega(\delta D_b + r D_v)}{kTR^3} \left\{ \frac{\left[1-(1-D)^{\frac{2}{3}}\right]}{3(1-D)^{\frac{2}{3}} - \left[1+(1-D)^{\frac{2}{3}}\right] en(1-D) - 3} \right\} P \quad , \qquad (14)$$

where

$\dot{\epsilon}_0$, σ_0, and n are material constants.

$\dot{\epsilon}$ and σ are effective strain rate and stress, respectively.

The creep densification rate in the initial stage is given by:

$$\dot{D}_{pL} = 5.3\left(D^2 D_0\right)^{\frac{1}{3}} \frac{\chi}{R} \left(\frac{\dot{\epsilon}_0}{\sigma_0^{\,n}}\right) \left(\frac{P_{eff}}{3}\right)^n \quad , \qquad (15)$$

where χ is the neck radius.

$\dot{D}_{pL}$ in the final stage is:

$$\dot{D}_{pL} = \frac{3}{2} \left(\frac{\dot{\epsilon}_0}{\sigma_0^{\,n}}\right) \left\{ \frac{D(1-D)}{\left[1-(1-D)^{\frac{1}{n}}\right]^n} \right\} \left(\frac{3}{2n} P\right)^n \quad . \qquad (16)$$

For tool steel: $n = 7.5$.

$$\frac{\dot{\epsilon}_0}{\sigma_0^{\,n}} = \frac{AbD_v}{kT\mu^{n-1}} \quad , \tag{17}$$

where

A = Dom constant = 1.5×10^{12}.

b = Burger's vector = 2.58×10^{-10} (m).

μ = shear modulus at the HIPing temperature.

$$\mu = \mu_0\left[1+\frac{(T-300)}{T_m}\left(\frac{T_m}{\mu_0}\frac{du}{dT}\right)\right] \quad , \tag{18}$$

where

μ_0 = shear modulus at 300°K = 8.1×10^4 (MPa).

T = HIPing temperature in °K.

T_m = melting temperature in °K.

$\frac{T_m}{\mu_0}\frac{du}{dT}$ = - 0.85 .

Again for a given material and specified HIPing temperature and pressure, $\dot{D}_{pL}$ in the two stages can be evaluated.

Other densification mechanisms such as the Nabarro-Herring and Coble creep have not been taken into account at the present time. The effects of different particle sizes are also neglected.

In conducting HIPing computations, the plastic yielding densification mechanism is considered to be instantaneous, and the density attained is treated as the starting value for the time-dependent densification mechanisms.

In the two densification stages, the total densification rate $\dot{D}_t$ is given by:

$$\dot{D}_t = \dot{D}_D + \dot{D}_{pL} \quad . \tag{19}$$

The approximate equations are used for $\dot{D}_D$ and $\dot{D}_{pL}$ at each stage.

Modeling Results

HIPing computation results are presented in two ways: (1) the densification rates are shown as a function of relative density, and (2) the relative density is shown as a function of time. The first case is a straight application of the equation for $\dot{D}_t$. In the second case, the equation for $\dot{D}_t$ is integrated by the Runge-Kutta method. Computer programs are developed to perform the calculations. Furthermore, the relative density as a function of time modeled under different conditions are plotted. Material parameters of H13 were employed in the modeling. The average particle size of 75 μm was used as a good approximation of the measured average particle size of H13 powder.

Figure 4 shows the computed relative density of H13 as a function of time at 1000°C under pressures of 100, 150, and 200 MPa. Under 100 MPa, the theoretical density was obtained after 33,785 s. When the pressure was doubled to 200 MPa, the time to reach theoretical density was decreased to 3,838 s, only 11% of that for 100 MPa. This indicates that increasing pressure greatly decreases the densification time.

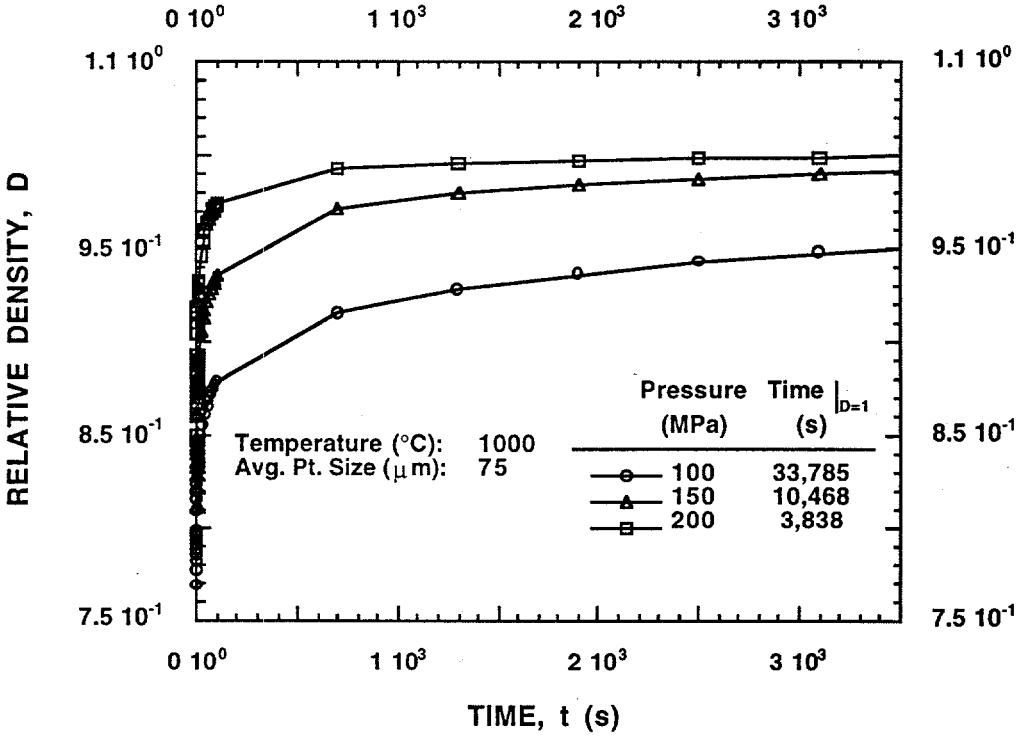

Fig. 4. Calculations of the relative density of H13 powder as a function of time at 1000°C under pressures of 100, 150, and 200 MPa.

Figure 5 shows the modeling results for a pressure of 100 MPa at 900, 1000, and 1100°C. When the temperature was increased from 900 to 1100°C, the time to reach theoretical density decreased from 36,000 to 7, 470, approximately only 21% of the former time.

Figure 6 shows the modeled particle size effect on the densification process. Obviously particle size has a great effect in the small size range, as the particle size increases, its effect on densification rate decreases.

Experimental Studies

Limited experimental studies were conducted based on the HIPing parameters predicted by the HIPing model. The results indicated that the model was capable of predicting the HIPing conditions that should be used. Figure 7 shows canned samples before and after HIPing.

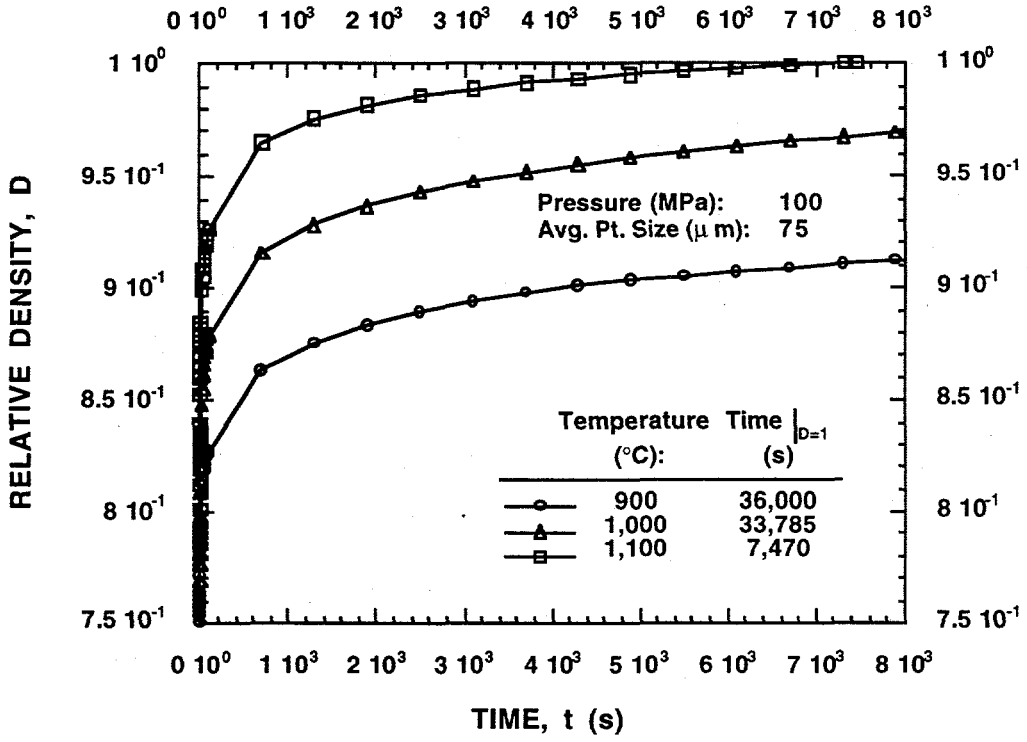

Fig. 5. Calculations of the relative density of H13 tool steel powder as a function of time at a pressure of 100 MPa at 900, 1000, and 1100°C.

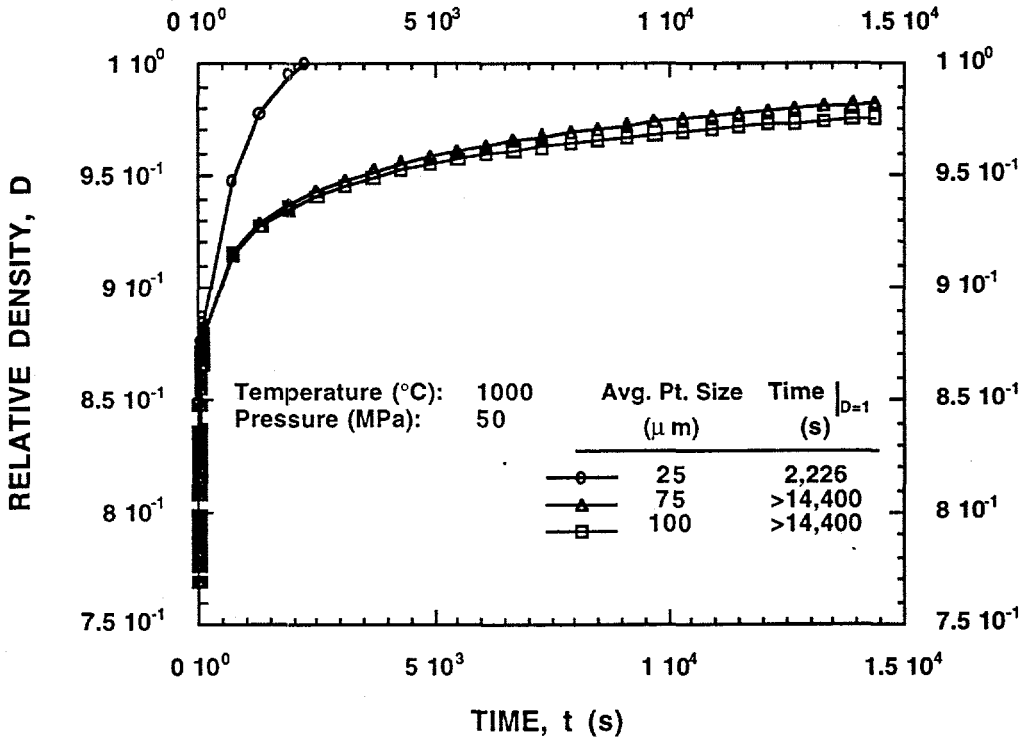

Fig. 6. Calculations of the relative density of H13 powder of different average grain sizes as a function of time for 100 MPa pressure and 1000°C temperature.

References

1. B. K. Lograsso, T. A. Lograsso, "Densification During Hot Isostatic Pressing", Proceedings of the Second International Conference on Hot Isostatic Pressing: Theory and Applications, p. 115-122, Gaithersburg. MD, 7-9 June 1989.

2. John J. Conway & Hohn H. Moll, "Current Status of Powder Metallurgy Near Net Shapes by Hot Isostatic Pressing", ASM International Third Conference on Near Net Shape Manufacturing, Pittsburgh, PA, USA, 27-29 September 1993.

3. L. E. Tidbury, R. M. Walker & G. D. Craven, "Development of Microstructural Features by Control of HIP Process Variables", Proceedings of the Second International Conference on Hot Isostatic Pressing: Theory and Applications, p. 83-89, Gaithersburg, MD, 7-9 June 1989.

4. E. Arzt, M. F. Ashby and K. E. Easterling, "Practical Applications of Hot-Isostatic Pressing Diagrams: Four Case Study", Metallurgical Transactions A, Vol. 14A, p. 211-221, February 1983.

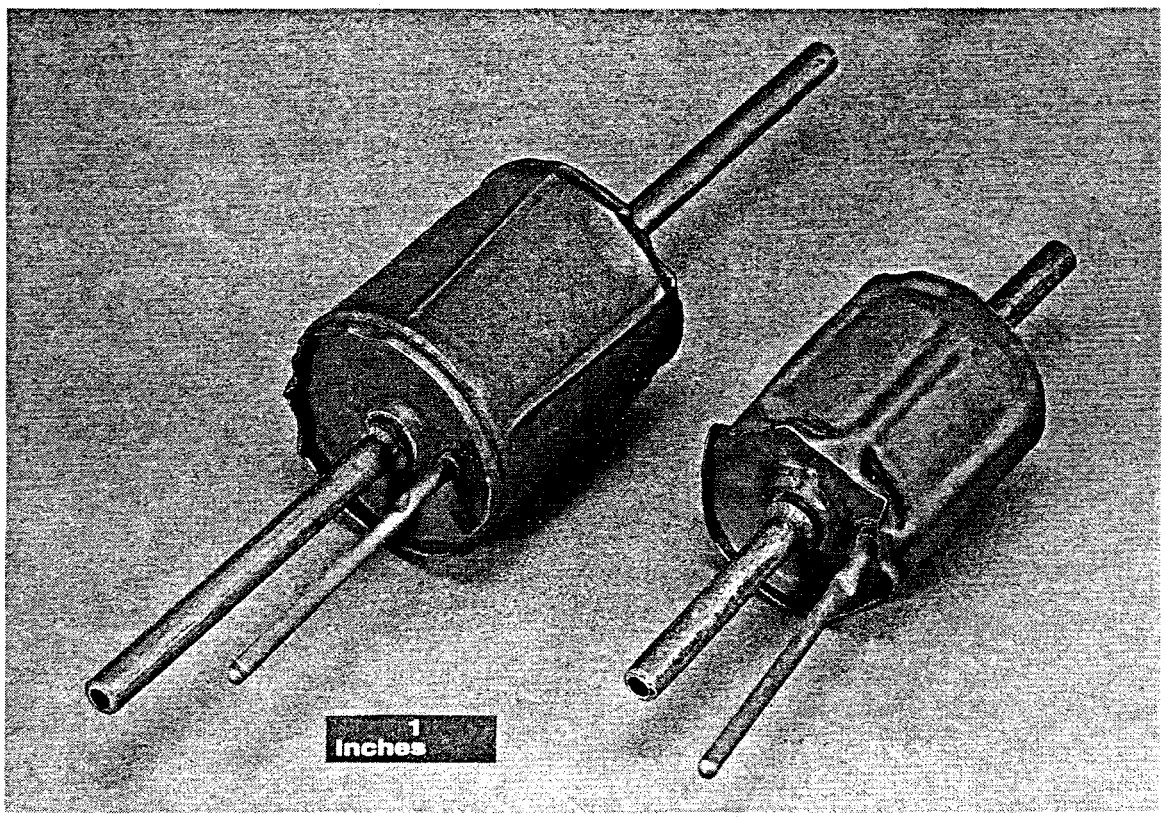

Fig. 7. Canned samples before and after HIPing.

5. John J. Wlassich & Roger B. Clough, "Investigation into a Grain Growth Model for Hot Isostatic Pressing", Proceedings of the Second International Conference on Hot Isostatic Pressing: Theory and Applications, p. 123-128, Gaithersburg. MD, 7-9 June 1989.

6. W. B. Li, M. F. Ashby, and K. E. Easterling, "On Densification and Shape Change During Hot Isostatic Pressing", Acta, Metall. Vol. 35, No. 12 p. 2831-2842, 1987.

7. R. J. Schaefer, "Intellegent Processing of Hot Isostatic Pressing", Thermal structures and Materials for High-Speed Flight, edited by Earl A. Thornton, Vol. 140 of Progress in Astronautics and Aeronautics, AIAA, Washington, DC, ISBN 1-56347-017-9, 1992.

8. A. H. Kahn, M. L. Mester & H. N. G. Wadley, "Eddy Current Techniques for Sample Dimension Measurements During Hot Isostatic Pressing", Proceedings of the Second International Conference on Hot Isostatic Pressing: Theory and Applications, p. 341-348, Gaithersburg. MD, 7-9 June 1989.

9. Alexander M. Laptev & Victor N. Samarov, "Theory of Hot Isostatic Pressing and Its Application for Calculation of Powder Compaction at High and Low Pressures", Compaction and Other Consolidation Processes, Advances in Powder Metallurgy & Particulate Materials, Vol. 2, p. 465-473, 1992.

10. R. J. henry & T. J. McCabe, "Computer Optimization of Near-Net-Shape Production of Powder Metallurgy Components", Proceeding of the Near-Net-Shape Manufacturing: Examining Competitive Processes Conference, Pittsburgh, PA, September 27-29, 1993.

11. S. Shima & M. Oyane, "Plasticity Theory for Porous Metals", Int. J. Mechanical science, Vol. 18, p. 285-291, 1976.

12. F. B. Swinkels, D. S. Wilkinson, E. Arzt & M. F. Ashby, "Mechanisms of Hot-Isostatci Pressing", Acta Metall. Vol. 31, No. 11, p. 1829-1840, 1983.

13. "Hot-Isostatic Pressing Diagrams: New Developments," A. S. Helle, K. E. Easterling, and M. F. Ashby, *Acta. Metall.*, Vol. 33, No. 12, p. 2163-2174, 1985.

Report of Inventions

There were no inventions developed under this agreement.

Commercialization Possibilities

The concepts evaluated in this project have immense potential if commercialized. However, further research and development will be required to commercialize the concepts. If such research is conducted, commercialization should be rapid as the base technology (hot isostatic processing) is well developed and widely available.

Plans for Future Collaboration

No plans have been made for future collaboration.

Conclusions

The object of this project was to investigate the manufacture die-casting dies with internal water cooling lines by hot isostatic pressing (HIPing) of H13 tool steel powder. The use of HIPing will allow the near-net-shape manufacture of dies and the strategic placement of water-cooling lines during manufacture. The production of near-net-shape dies by HIPing involves the generation of HIPing diagrams, the design of the can that can be used for HIPing a die with complex details, strategic placement of water-cooling lines in the die, computer modeling to predict movement of the water lines during HIPing, and the development of strategies for placing water lines in the appropriate locations. The results presented include a literature review, particle analysis and characterization of H13 tool steel powder, and modeling of the HIPing process.

The results of the powder characterization and modeling studies undertaken in this project suggested the feasibility of production of near-net-shaped dies by HIPing. However, further experimental trials involving the design of the can that can be used for HIPing a die with complex details and the strategic placement of water-cooling lines in the die is needed. Since the water lines may move during HIPing, computer modeling must be used to predict movement of the water lines and devise strategies for placing water lines in the appropriate locations. Unfortunately, the level of effort allowed in this CRADA did not allow further experimental and computer trials.

INTERNAL DISTRIBUTION

1. R. A. Bradley
2. D. F. Craig
3. P. L. Gorman
4-5. D. R. Hamrin
6. H. W. Hayden, Jr.
7. L. L. Horton
8. A. J. Luffman
9. K. Luk
10. T. L. Payne
11. W. Ren
12. V. K. Sikka
13. C. A. Valentine
14-17. S. Viswanathan
18. Central Research Library
19. Document Reference Section
20. Laboratory Records - RC
21. ORNL Patent Section
22-23. Y-12 Central Files

EXTERNAL DISTRIBUTION

24-25. Office of Scientific and Technical Information, P.O. Box 62, Oak Ridge, TN 37831
26. DOE Work For Others, ER-113, P.O. Box 2001, Oak Ridge, TN 37831
27. DOE, Oak Ridge Operations, P.O. Box 2001, Oak Ridge, TN 37831-6269
28. S. J. Barish, Department of Energy, ER-32, 19901 Germantown Rd., Germantown, MD 20874-1290
29. W. M. Polansky, Department of Energy, ER-32, 19901 Germantown Rd., Germantown, MD 20874-1290